Toxicology Letters 383 (2023) 54–63

Contents lists available at ScienceDirect

Toxicology Letters

journal homepage: www.journals.elsevier.com/toxicology-letters

Ribotoxin deoxynivalenol induces taurocholic acid malabsorption in an in vitro human intestinal model

Jingxuan Wang *, Bas Sijs, Wouter Bakker, Laura de Haan, Hans Bouwmeester

Division of Toxicology, Wageningen University and Research, Stippeneng 4, 6708 WE Wageningen, the Netherlands

ARTICLE INFO

Editor: Dr. Angela Mally

Keywords:
Bile acid malabsorption
Deoxynivalenol
Inflammation
Ribotoxin

ABSTRACT

The trichothecene toxin deoxynivalenol (DON) is a ribotoxic mycotoxin that contaminates cereal-based food. DON binds to ribosomes, thereby inhibiting protein translation and activating stress mitogen-activated protein kinases (MAPK). The activation of MAPK induces pro-inflammatory cytokine production. Emerging evidence showed that DON decreased bile acid reabsorption and apical sodium-dependent bile acid transporter (ASBT) expression in Caco-2 cell layers. We hypothesized that the effect of DON on decreased ASBT mRNA expression is regulated via pro-inflammatory cytokines. We observed that MAPK inhibitors prevented DON to induce IL-8 secretion and prevented the DON-induced downregulation of ASBT mRNA expression. However, DON-induced taurocholic acid (TCA) transport reduction was not prevent by the MAPK inhibitors. We next observed a similarity between the activity of the non-inflammatory ribotoxin cycloheximide and DON to decrease TCA transport, which is consistent with their common ability to inhibit protein synthesis. Together, our results suggest that DON-induced TCA malabsorption is regulated by MAPK activation-induced pro-inflammatory cytokine production and protein synthesis inhibition, both of which are initiated by DON binding to the ribosomes which therefore is the molecular initiating event for the adverse outcome of bile acid malabsorption. This study provides insights into the mechanism of ribotoxins-induced bile acid malabsorption in human intestine.

1. Introduction

The trichothecene toxin deoxynivalenol (DON) is a ribotoxic mycotoxin that is frequently observed in cereal grains. The Joint FAO/WHO Expert Committee on Food Additives (JECFA) estimated the dietary exposure to DON to vary from 0.2 to 14.5 μg/kg bw per person per day across the different global regions. For Europe the average exposure was 1.4 μg/kg bw per day (JECFA, 2011). European Food Safety Authority (EFSA) established a tolerable daily intake (TDI) of 1.0 μg/kg bw per day for DON (EFSA, 2017). DON is known to cause a variety of toxic effects in humans and animals (EFSA, 2017; Maresca, 2013; Sergent et al., 2006). The toxic effect of DON is initiated by the binding of DON to ribosomes, thereby inhibiting protein translation and reducing the protein level in the cells. In addition, the binding of DON to ribosomes also induces ribotoxic stress (EFSA, 2017; Pestka, 2010). Ribotoxic stress results in the activation of the mitogen-activated protein kinases (MAPK) and their downstream transcription factors like nuclear factor-kB (NF-kB) (Ge et al., 2020; Laskin et al., 2002). The activation of these transcription factors results in inflammation induced by DON (Mishra et al., 2014; Zhang et al., 2020). The intestine is the main target tissue of DON (Maresca and Fantini, 2010). Chronic ingestion of DON at human dietary levels caused intestinal inflammation in mice (Vignal et al., 2018). DON induced persistent intestinal inflammation in porcine intestinal epithelial cells (IPEC-1) and porcine jejunal explants, with a significant increase in the mRNA encoding the pro-inflammatory cytokine IL-8 (Cano et al., 2013). Increased IL-8 secretion and MAPK activation were also found in human intestinal Caco-2 cells exposed to DON (Van De Walle et al., 2008).

Intestinal inflammation is associated with a decreased transport of bile acids across the intestinal epithelium in humans (Jia et al., 2018). Bile acids are synthesized in the liver and secreted in the intestinal lumen via the bile. Intestinal bile acids are reabsorbed by intestinal epithelial cells and circulated back to the liver via the portal vein, where they are recycled for another entero-hepatic cycle (Alrefai and Gill,

Abbreviations: DON, deoxynivalenol; JECFA, Joint FAO/WHO Expert Committee on Food Additives; MAPK, mitogen-activated protein kinases; ASBT, apical sodium-dependent bile acid transporter; OST, organic solute transporter; TCA, taurocholic acid; IBD, inflammatory bowel disease; BCA, bicinchoninic acid; LOQ, limit of quantitation.

* Corresponding author.
E-mail address: jingxuan.wang@wur.nl (J. Wang).

https://doi.org/10.1016/j.toxlet.2023.06.001
Received 11 March 2023; Received in revised form 23 May 2023; Accepted 10 June 2023
Available online 12 June 2023

2007). The efficient bile acid reabsorption depends on the proper functioning of bile acid active transporters in the intestine (Dawson et al., 2009). The apical sodium-dependent bile acid transporter (ASBT) absorbs bile acids form the lumen of the small intestine across the apical brush border membrane, while the basolateral organic solute transporter (OST) mediates the efflux of bile acids out of the intestinal epithelial cells (Dawson et al., 2009). OST has a low affinity but a high capacity for transporting bile acids whereas ASBT has a high affinity for bile acids and can be saturated by low concentrations of bile acids (Balakrishnan et al., 2006; Suga et al., 2019). These kinetics imply that the expression of ASBT instead of OST controls the bile acid reabsorption rate in the intestine.

Decreased expression of bile acid transporter ASBT was observed in patients with inflammatory intestinal disease (IBD) (Jahnel et al., 2014). IBD patients suffer from increased pro-inflammatory cytokine production (Reimund et al., 1996). Inflammatory cytokines IL-1 and TNF-α repress rat bile acid transporter ASBT expression in vivo (Chen et al., 2002). This was confirmed in human Caco-2 cells, which suggests that pro-inflammatory cytokines are able to decrease bile acid transport across differentiated Caco-2 cell layers by decreasing the ASBT expression (Neimark et al., 2006). Emerging evidence showed that DON decreased bile acid transport and transporter ASBT expression in Caco-2 cell layers (Wang et al., 2022). Considering that DON induces inflammation via activating MAPK pathways in the intestine, it is hypothesized that the previously reported effect of DON on decreased bile acid reabsorption may be regulated by MAPK pathways.

The purpose of this study was to explore whether the effect of DON on decreased bile acid reabsorption and bile acid transporter ASBT expression was regulated by MAPK activation mediated inflammation in Caco-2 cells. To test our hypothesis, Caco-2 cell layers grown in Transwells were exposed to DON. MAPK inhibitors were used to inhibit the MAPK pathway activation and thereby inhibiting the pro-inflammatory response of Caco-2 cells following DON exposure. Pro-inflammatory cytokines were quantified by ELISA, ASBT mRNA expression was quantified by RT-qPCR. Taurocholic acid (TCA) is one of the conjugated bile acids that has long been used as model bile acid for transport studies (Heubi et al., 1982; Li et al., 2018). TCA transport was quantified by using an LC-MS/MS method.

2. Materials and methods

2.1. Cell culture

Human colon carcinoma Caco-2 cells (passage number 10–30) were grown at 37 °C with 5 % CO_2 in Minimum Essential Medium (MEM) (Gibco BRL, Breda, Netherlands), supplemented with 20 % heat-inactivated fetal bovine serum, 1 % pyruvate and 1 % penicillin/streptomycin/glutamine (Gibco BRL). Cells were subcultured at 50–70 % confluence by using 0.05 % trypsin (Gibco BRL). Caco-2 cells were seeded at 1×10^5 cells/insert in 12-well polycarbonate membrane inserts (Corning Costar, Schnelldorf, Germany) or polyethylene terephthalate membrane inserts (Greiner bio-one, Kremsmunster, Austria) with 0.4 μm pore size and maintained in culture for 18–20 days. The culture medium was changed every other day.

2.2. Caco-2 cell layer exposure

Different exposure conditions where used for different experiments. The pro-inflammatory cytokine TNFα 0–800 pg/ml (Novus, CO, USA) was used to obtain inflamed Caco-2 cell layers (adapted from Sonnier et al., 2010). The concentration of DON (Sigma-Aldrich, MO, USA) was 2.5 μM. This concentration is related to realistic human intake and non-cytotoxic to Caco-2 cell layers (Wang et al., 2022). To inhibit the MAPK activation, the Caco-2 cell layers were co-exposed to 20 mM MAPK p38 inhibitor SB203580, 20 mM JNK1/2 inhibitor SP600125 and 20 mM ERK1/2 inhibitor U0126 (Sigma-Aldrich; adapted from Zhang et al., 2020). To specifically block protein synthesis, 0–10 μM cycloheximide was exposed in Caco-2 cell layers. All the exposures were continued for 48 h to ensure the degradation of ASBT protein (Xia et al., 2004).

2.3. TCA transport assay

18–20 days cultured Caco-2 cell layers were pre-exposed to 0.5 % DMSO, 2.5 μM DON (Sigma-Aldrich), MAPK inhibitors, TNFα or cycloheximide for 48 h depending as described above. The exposure medium was then removed and the apical Caco-2 cell layers were gently rinsed with Hank's balanced salt solution (Gibco BRL) supplemented with 10 mM HEPES (transport medium). After a 30-min incubation in transport medium, 5 nmol TCA (Sigma-Aldrich) in 0.5 ml transport medium was added to the apical compartment. After incubating for 0, 30, 60, 90 or 120 mins, the amount of TCA was measured in the basolateral or apical compartment by using LC/MS/MS.

2.4. Profiling of primary bile acids by LC/MS/MS

Chromatographic separation of TCA was adapted from our previous study (Wang et al., 2022) and carried out by using the Shimadzu 8045 System (Kyoto, Japan). Aliquots of samples (1 μL) were injected by using an autosampler. The analytes were separated using a phenomenex 00B-4475-AN (50 mm × 2.1 mm × 1.7 μm × 100 Å, Kinetex C18) analytical column with a Phenomenex AJ0–8782 guard column at a column temperature of 40 °C. The mobile phase consisted of MilliQ water with 0.01 % formic acid (A) and methanol with 50 % acetonitrile (B) using a starting gradient that contained 30 % B, linearly increasing to 70 % B at 10 min, then stable with 98 % B at 11.0–18.0 min. As a last step the percentage of B was reduced to 30 % at 19–25 min. The flow rate was set at 0.4 ml/min. The optimal Electrospray ionization (ESI) Mass Spectrometry (MS) is used in negative-ion mode (Shimadzu). The ESI source parameters were as follows: nebulizer gas flow 3 L/min; heating gas and drying gas flow 10 L/min; interface temperature at 300 ℃; desolvation line (DL) temperature at 250 ℃; and heat block temperature at 400 ℃. The multiple reaction monitoring (MRM) and selective ion monitoring (SIM) modes were used for quantification. Data were collected and processed by using the LabSolutions software Version 5.6 (Shimadzu).

2.5. Fluorescein transport

To ensure the paracellular transport is at the same level among different exposure experiments, the integrity of Caco-2 cell layers after TCA transport was assessed by using Fluorescein transport measurements. After 120 mins of TCA transport, the transport medium with TCA was removed and the apical Caco-2 cell layers were gently rinsed with transport medium. Next, 25 nmol Fluorescein (Sigma-Aldrich) in 0.5 ml transport medium was added to the apical cell compartment. After 1 h of incubation the amount of fluorescence was measured in the basolateral compartment with SpectraMax M2 microplate reader. The excitation and emission wavelengths were 490 and 520 nm, respectively. The data are presented as the percentage of solvent control group.

2.6. mRNA hextraction and RT-qPCR analysis

Following exposure of Caco-2 cell layers to different treatments (Section 2.2), RNA was isolated using the QIAshredder and RNeasy® mini kit (Qiagen, Hilden, Germany) according to the manufacturer's instructions. The quantity and quality of isolated mRNA was confirmed by Nanodrop (ND-1000; ThemoScientific, MA, USA). Subsequently cDNA was generated from 300 ng of total RNA using the QuantiTect® reverse transcription kit (Qiagen). RT-qPCR analysis was carried out using the Rotor-Gene® SYBR® Green PCR kit and the Rotor-Gene® 6000 cycler according to the manufacture's handbook. The human-specific

ASBT, TNFα and β-actin primers were commercially available from QuantiTect® Primer Assays (Qiagen). The IL-1β and IL-8 primer (Biolegio, Nijmegen, Netherlands) was synthesized according to the sequence (F:- GTGGCAATGAGGATGACTTGTTC, R:- TAGTGGTGGTCGGAGATTCGTA) and (F:- CTGATTTCTGCAGCTCTGTG, R:- GGGTGGAAAGGTTTGGAGTATG). The efficiency of the primers was checked prior to sample measurement. Values were quantified using the comparative threshold cycle method. Target gene mRNA expression was normalized to β-actin (Pfaffl, 2001). The data are presented as percentage of solvent control group.

2.7. Cytokine quantification

For cytokine quantification, medium was collected from the apical compartment at 6 or 48 h after exposure. The amount of TNFα, IL-1β or IL-8 was quantified by the Enzyme-Linked Immune-Sorbent Assay (ELISA) according to the manufacturer's instructions (Biolegend, CA, USA). The Limit of Quantitation (LOQ) for TNFα, IL-1β and IL-8 are 7.8, 2.0 and 15.6 pg/ml respectively, while the Limit of Detection (LOD) is for TNFα, IL-1β and IL-8 are 2, 0.5 and 2 pg/ml respectively according to the manufacturer's instructions (Biolegend, CA, USA).

2.8. Protein quantification

Following exposure to DON or cycloheximide Caco-2 cells were harvested by using M-PER mammalian extraction buffer (Thermo Fisher, MA, USA) supplemented with phosphatase and phosphatase inhibitor cocktail (Thermo Fisher) on ice and then centrifuged to obtain the total protein. The protein was quantified by the Bicinchoninic Acid (BCA) protein assay according to the manufacturer's instructions (Thermo Fisher).

2.9. Statistics

Data are presented as the means of three biological replicates ± SD. Statistical analysis was performed by Student t test or ANOVA followed by the Dunnett test. $p < 0.05$ was considered as statistically significant. If detected values are <LOQ and >LOD, half LOQ was used in the statistical evaluation. All data were analysed with SPSS Version 17.0 (SPSS Inc., Chicago, IL, USA).

3. Results

3.1. Pro-inflammatory cytokine exposure decreases TCA transport across Caco-2 cell layers

TNFα and IL-1β downregulate ASBT mRNA expression in Caco-2 cells (Neimark et al., 2006). To assess the effect of these pro-inflammatory cytokines on TCA transport, 18–20 days cultured Caco-2 cells were stimulated by TNFα to obtain inflamed Caco-2 cell layers (Sonnier et al., 2010). Next, we added 5 nmol TCA to the apical compartment of the inflamed Caco-2 cell layers and after 120 mins transport measured the basolateral TCA concentrations. Fig. 1 A, shows that TCA transport was dose-dependently decreased to 0.4 ± 0.1 nmol following 800 pg/ml TNFα exposure compared to 0.7 ± 0.1 nmol following solvent exposure. After TCA transport, the barrier integrity of the Caco-2 cell layers was measured by the Fluorescein transport assay. The fluorescein paracellular permeability remained the same and lower than 5 % of the total fluorescein for all TNFα exposure groups. (Fig. 1B).

3.2. DON induces pro-inflammatory cytokine production in Caco-2 cell layers

To assess if DON induced inflammation in Caco-2 cell layers, we exposed 18–20 days cultured Caco-2 cell layers to 2.5 μM DON. Pro-inflammatory cytokines TNFα, IL-1β and IL-8 mRNA expression and protein secretion were quantified by RT-qPCR and ELISA following 6 and 48 h of DON exposure. As shown in Fig. 2 A, no significant increases of TNFα and IL-1β mRNA expression was observed following 6 or 48 h DON exposure compared to solvent control. The IL-8 mRNA expression increased to 529.9 ± 31.7 % and 503.3 ± 86.4 % of the solvent control at 6 or 48 h DON exposure respectively.

The TNFα and IL-1β secretion was lower than the quantitation limit (7.8 pg/ml and 2.0 pg/ml respectively) at both 6 and 48 h following DON exposure (data not shown). The IL-8 secretion was below the ELISA quantitation limit (15.6 pg/ml) at 6 h for both the solvent control and

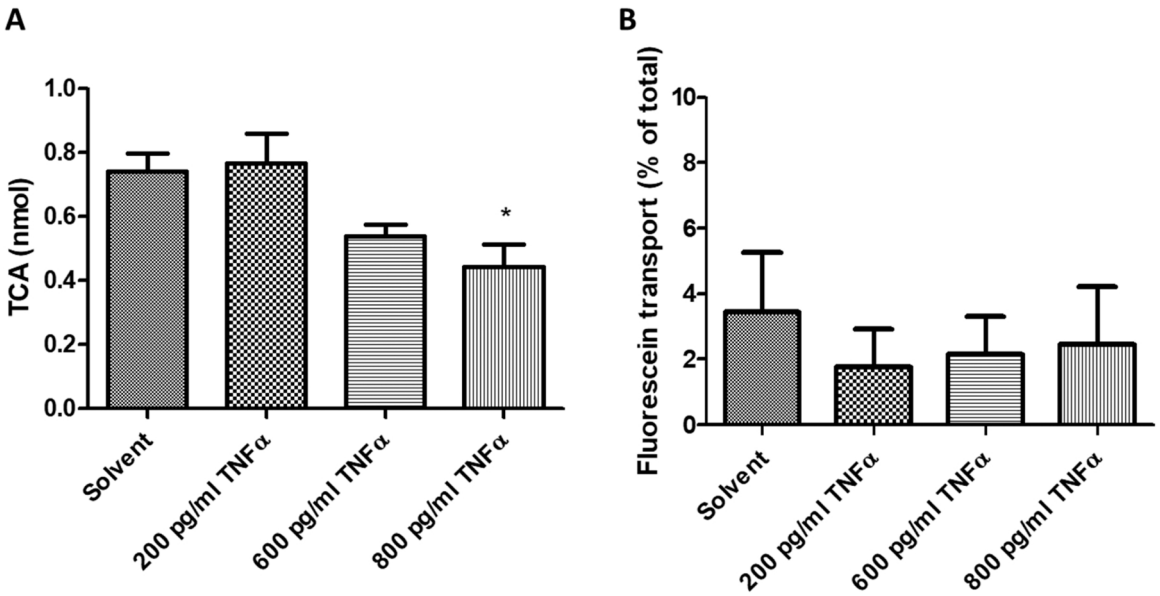

Fig. 1. The pro-inflammatory cytokine TNFα decreases TCA transport across Caco-2 cell layers. (A) 18–20 day cultured Caco-2 cell layers were incubated with 0–800 pg/ml TNFα for 48 h before exposure to 5 nmol TCA in 0.5 ml apical transport medium. TCA transport from the apical to basolateral compartment was determined at 120 mins. (B) After TCA transport, the barrier integrity and paracellular permeability was measured by Fluorescein transport assay. Data were expressed as mean ± SD, n = 3. Statistical analysis was performed by ANOVA followed by the Dunnett test. * : significantly different from the solvent control group ($p < 0.05$).

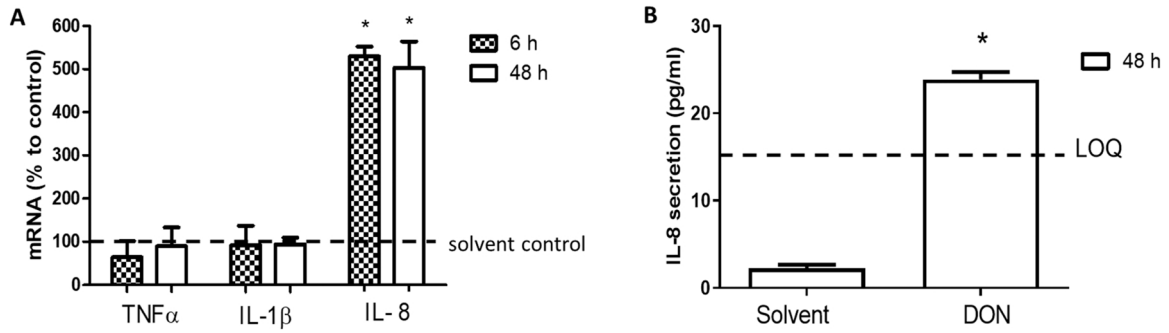

Fig. 2. DON induces IL-8 production in Caco-2 cell layers. (A) The mRNA expression of TNFα, IL-1β and IL-8 in Caco-2 cell layers following exposure to 2.5 μM DON for 6 or 48 h was analyzed by RT-qPCR and compared to the level of the solvent (0.5 % DMSO), which was set at 100 %. (B) The IL-8 secretion in the apical compartment was quantified by ELISA following 2.5 μM DON exposure for 48 h. Data were expressed as mean ± SD, n = 3. Statistical analysis was performed by Student t test. * : significantly different from the solvent control group ($p < 0.05$). LOQ: Limit of Quantitation (see materials and methods).

DON exposure (data not shown). It increased to 23.9 ± 1.5 pg/ml following DON exposure which was significantly different compared to the solvent control at 48 h (Fig. 2B).

3.3. MAPK inhibitors prevent the effect of DON on IL-8 secretion and ASBT mRNA expression in Caco-2 cell layers

DON induces inflammation via MAPK pathways (Pestka et al., 2004). Here we used MAPK pathway inhibitors to inhibit the inflammatory response following DON exposure. 18–20 days cultured Caco-2 cell layers were exposed to 2.5 μM DON and/or MAPK inhibitors for 48 h. IL-8 secretion was determined by ELISA. As shown in Fig. 3 A, DON increased IL-8 secretion to a level of 24.7 ± 9.5 pg/ml which was significantly higher compared to the IL-8 secretion in the solvent control. Co-exposure of the Caco-2 cell layers to DON and MAPK pathway inhibitors prevented IL-8 secretion as IL-8 excretion could no longer be detected. The results suggested that DON cannot cause inflammation responses upon MAPK inhibition.

Next, we quantified ASBT mRNA expression by RT-qPCR following DON and/or MAPK inhibitors exposure (Fig. 3B). DON exposure downregulated the ASBT mRNA expression in the Caco-2 cell layers to 50.3 ± 18.0 % of the non-exposed control cells. The ASBT mRNA expression following exposure to MAPK inhibitors was comparable to that in control cells (no significant difference compared to control). The co-exposure of DON and MAPK inhibitors increased ASBT mRNA expression to 171.7 ± 37.8 % of control. These results indicate that the downregulation of ASBT mRNA expression by DON was prevented by co-exposure with MAPK inhibitors. The increased ASBT mRNA expression following DON+MAPK inhibitors exposure suggests that in addition to the MAPK pathway, there is an additional MAPK-independent pathway involved affecting ASBT mRNA expression upon DON exposure.(Fig. 4).

3.4. MAPK inhibitors do not prevent the effect of DON on TCA transport

Next, we assessed if MAPK inhibitors prevent the effect of DON on TCA transport by Caco-2 cell layers. 18–20 days cultured Caco-2 cells were exposed to 2.5 μM DON and/or MAPK inhibitors for 48 h. Then, the exposure medium was removed and 5 nmol TCA was added in 0.5 ml apical transport medium. TCA was quantified in the basolateral

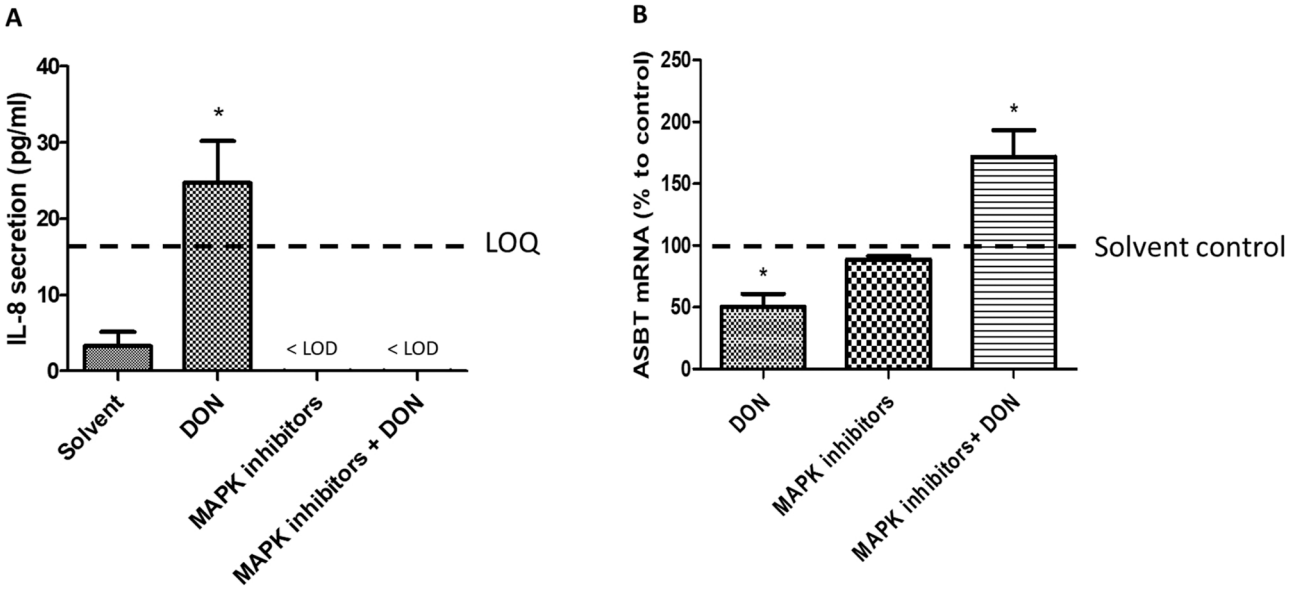

Fig. 3. MAPK inhibitors prevent the effect of DON on increased inflammation and on decreased ASBT mRNA expression in Caco-2 cell layers. (A) 18–20 days cultured Caco-2 cell layers were exposed to DMSO, 2.5 μM DON or/and MAPK inhibitors (co-exposure of 20 mM SB203580, 20 mM SP600125 and 20 mM U0126) for 48 h. The IL-8 secretion in the apical compartment was quantified by ELISA. (B) The mRNA expression of ASBT in Caco-2 cell layers was analyzed by RT-PCR and compared to the level of the solvent control (0.5 % DMSO), which was set at 100 %. Data were expressed as mean ± SD, n = 3. Statistical analysis was performed by ANOVA followed by the Dunnett test. * : significantly different from the solvent control group ($p < 0.05$). LOQ: Limit of Quantitation, LOD: Limit of Detection (see materials and methods).

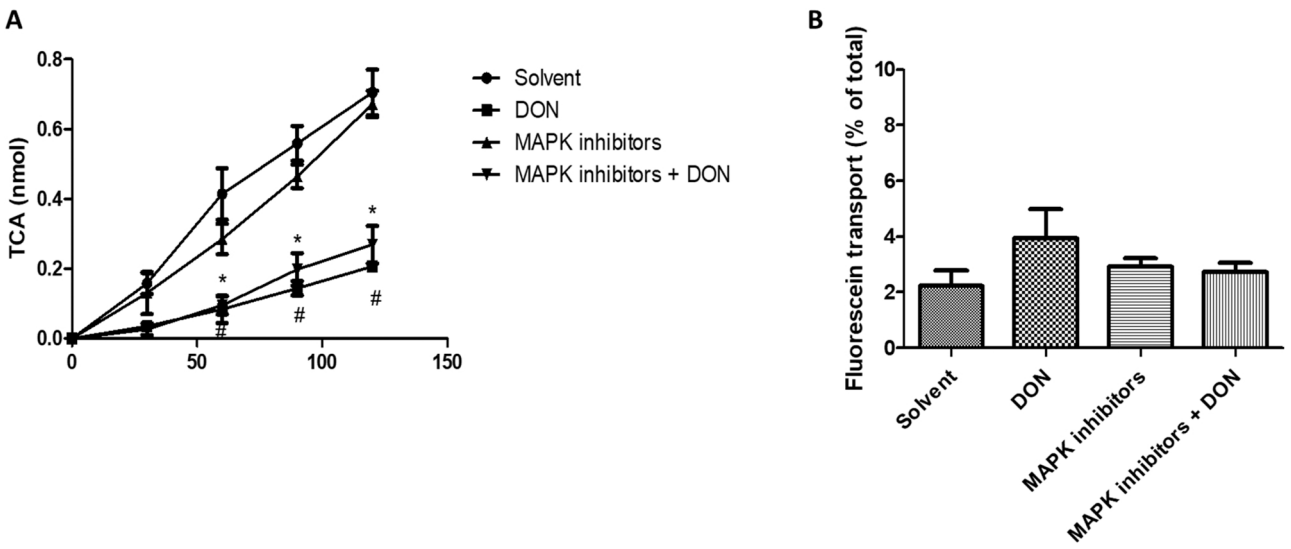

Fig. 4. MAPK inhibitors do not eliminate the effect of DON on TCA transport. (A) 18–20 days cultured Caco-2 cell layers were exposed to DMSO, 2.5 μM DON and/or MAPK inhibitors (consisting of a mixture of 20 mM SB203580, 20 mM SP600125 and 20 mM U0126) for 48 h before exposure to 5 nmol TCA in 0.5 ml apical transport medium. TCA transport from the apical to basolateral compartment was determined during 120 mins. (B) After TCA transport, the paracellular fluorescein transport across Caco-2 cell layers was quantified by the Fluorescein transport assay. Data were expressed as mean ± SD, n = 3. Statistical analysis was performed by ANOVA followed by the Dunnett test. * : significantly different from the solvent control group ($p < 0.05$).

compartment following 120 mins of apical TCA exposure. As shown in Fig. 5 A, MAPK inhibitors pre-exposure did not significantly influence TCA transport compared to control (0.4 ± 0.1, 0.6 ± 0.09 and 0.7 ± 0.1 nmol at 60, 90 and 120 mins respectively). A significantly lower amount of TCA was detected in the basolateral compartment of the DON exposed Caco-2 cultures at 60, 90 and 120 mins (0.1 ± 0.07, 0.1 ± 0.04 and 0.2 ± 0.02 nmol respectively) compared to the solvent control. Interestingly, the co-exposure of the Caco-2 cell layers to DON in the presence of MAPK inhibitors did not eliminate the decreasing effect of DON on TCA transport. The TCA detected in the basolateral compartment of the co-exposure group was 0.1 ± 0.04, 0.2 ± 0.08 and 0.3 ± 0.09 nmol at 60, 90 and 120 mins respectively. After TCA transport, the Caco-2 cell layers were exposed to fluorescein. There was no significant difference of fluorescein transported across solvent, DON, MAPK inhibitors or DON+MAPK inhibitors (pre)exposed Caco-2 cell layers during 1-hour incubation (2.2 ± 1.0 %, 4.0 ± 1.8 %, 2.9 ± 0.5 % or 2.7 ± 0.6 % of the total fluorescein respectively). The results for fluorescein indicate that the paracellular transport among the different (pre)exposure groups was similar. Therefore the observed difference in TCA transport can be ascribed to different transcellular TCA transport among pre-exposure groups.

3.5. Cycloheximide inhibits the protein synthesis and decreases TCA transport in Caco-2 cell layers

Upon DON exposure, the upstream event of MAPK activation is ribosome binding, which results in the inhibition of protein synthesis (Pestka, 2010). We confirmed that DON inhibited protein synthesis in Caco-2 cell layers (Supplementary Material Fig. S1). To study if an effect on protein synthesis can indeed result in decreased TCA transport in Caco-2 cell layers, we tested the effect of cycloheximide on protein synthesis and TCA transport. Similar to DON, cycloheximide inhibits protein synthesis by binding to the ribosome (Schneider-Poetsch et al., 2010; Siegel and Sisler, 1963). Cycloheximide dose-dependently decreased the protein content in Caco-2 cells. The protein content significantly decreased to 89.0 ± 3.5 % following 0.05 μM cycloheximide exposure (Fig. 5 A). However, unlike DON, cycloheximide did not increase IL-8 secretion up to 10 μM cycloheximide exposure in Caco-2 cell layers (Fig. 5B). Next, we studied the effect of cycloheximide on TCA transport across Caco-2 cell layers. After 120 mins TCA exposure, the TCA amount in basolateral compartment significantly decreased to 0.6 ± 0.1 nmol to 0.3 ± 0.1 nmol following 0.05–10 μM cycloheximide exposure compared to the solvent control (1.0 ± 0.2 nmol). The paracellular fluorescein transport increased up to 2.7 ± 3.3 % following 10 μM cycloheximide exposure, which was not statistically different from the solvent control (0.1 ± 3.9 %) (Fig. 5 D). These results show that the non-inflammatory ribotoxin cycloheximide inhibits TCA transport, a result that is consistent with the common ability of DON and cycloheximide to inhibit protein synthesis.

4. Discussion

Based on the collective results shown we have postulated a mode of action of ribotoxin DON on TCA transport across a Caco-2 cell layers (Fig. 6). We first demonstrated that TCA transport was decreased across pro-inflammatory cytokine TNFα induced inflamed Caco-2 cell layers. Next, we confirmed that DON exposure induced inflammation via MAPK pathways in Caco-2 cell layers, as indicated by an increased IL-8 secretion inhibited by MAPK inhibitors. Moreover, we found that MAPK inhibitors prevented the DON induced downregulation of ASBT mRNA expression. However, the decreased effect of DON on ASBT-mediated TCA transport was not affected by MAPK inhibitors. Finally, we found that the non-inflammatory ribotoxin cycloheximide inhibited protein synthesis and reduced TCA transport without increasing IL-8 secretion. Together, these results indicate that the DON-induced TCA malabsorption is regulated by MAPK activation induced inflammatory cytokine production and protein synthesis inhibition, both of which are initiated by the ribosomes binding activity of DON which therefore is the molecular initiating event for the adverse outcome of bile acid malabsorption in the intestine.

Our results show that the expression of the pro-inflammatory genes coding for IL-8 and the IL-8 protein secretion from Caco-2 cells increased following 2.5 μM DON exposure, while the mRNA and protein secretion of TNFα and IL-1β were not increased. These results are consistent with findings from earlier studies, showing no detectable TNFα and IL-1β mRNA increases and protein secretion in 8-days cultured Caco-2 cells following 1.5 μM DON exposure, whereas the IL-8 mRNA gene expression and protein secretion were significant increased (Kadota et al., 2013). IL-8 is a chemoattractant cytokine produced by epithelial cells and specifically targets neutrophils, which does not affect epithelial cells

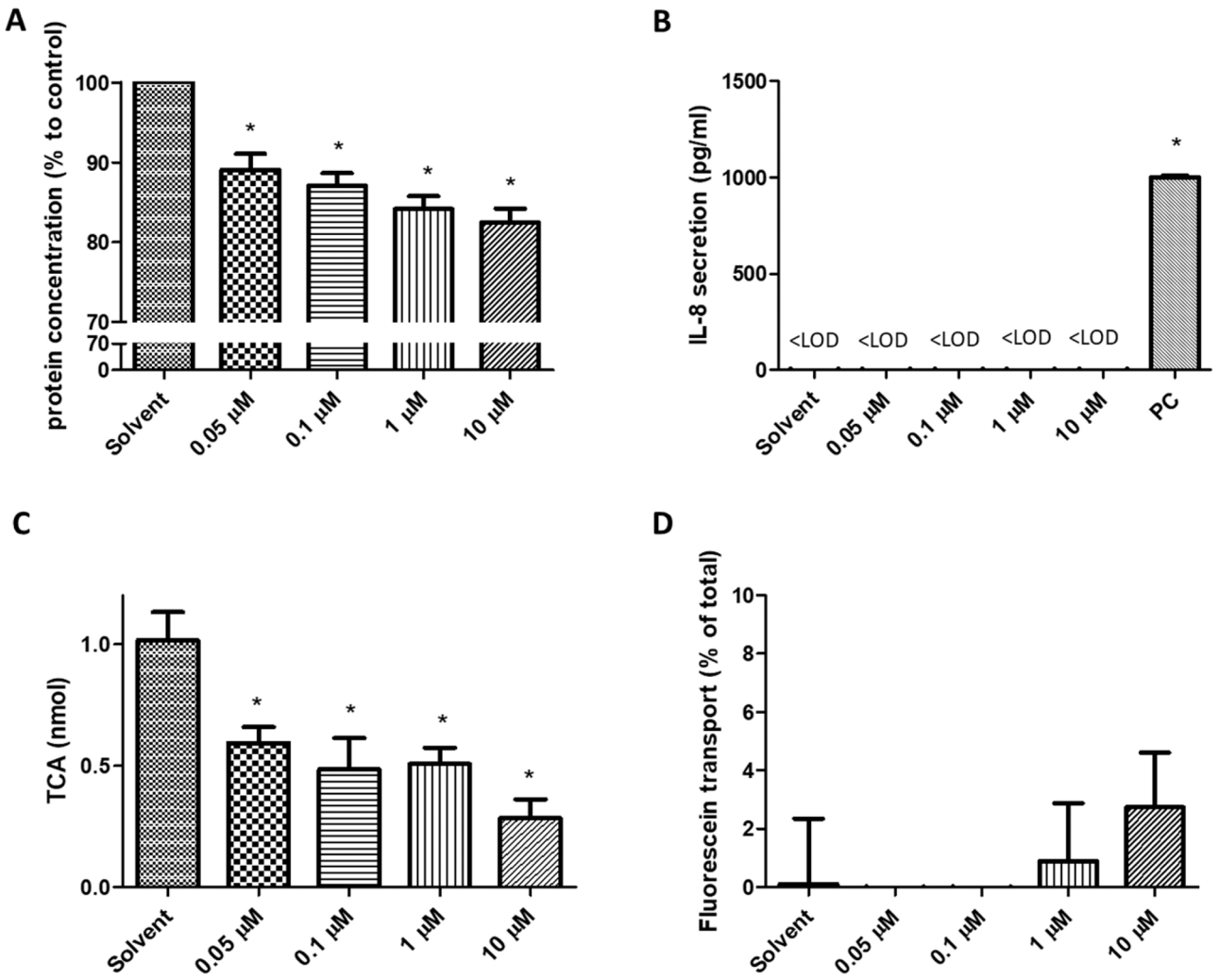

Fig. 5. Cycloheximide inhibits the protein synthesis and decreases TCA transport in Caco-2 cell layers. (A)18–20 day cultured Caco-2 cell layers were incubated with cycloheximide (0–10 μM) for 48 h. The protein content was quantified by BCA assay. (B) The IL-8 secretion in the apical compartment was quantified by ELISA. 25 ng/ml IL-1β was used as positive control. (C) After cycloheximide exposure, the Caco-2 cell layers were exposure to 5 nmol TCA in 0.5 ml apical transport medium. TCA transport from the apical to basolateral compartment was determined at 120 mins. (D) After TCA transport, the paracellular fluorescein transport across Caco-2 cell layer was quantified by the Fluorescein transport assay. Data were expressed as mean ± SD, n = 3. Statistical analysis was performed by ANOVA followed by the Dunnett test. * : significantly different from the solvent control group ($p < 0.05$).

themselves (Schuerer-Maly et al., 1994). The secretion of IL-8 has long been recognized as a sensitive marker for indicating inflamed states in differentiated Caco-2 cells whereas other cytokines are less sensitive (Van De Walle et al., 2010). Ribosomes are the main target of DON in cells. Binding of DON to ribosome recruits double stranded RNA activated protein kinase (PKP) and hematopoietic cell kinase (HCK) (Hou et al., 2021). These two kinases function as sensors of ribotoxic stress and activate several MAPK pathways, including JNK, p38 and ERK1/2 (Payros et al., 2016). Dose-dependent activation of JNK, p38 and ERK1/2 is observed in Caco-2 cells following DON exposure (Sergent et al., 2006). Similar results are confirmed in RAW 264.7 and IPEC-J2 cell lines (Chung et al., 2003; Zhang et al., 2020). These MAPK pathways mediate the inflammatory response of DON exposure, with active downstream transcription factors like c-fos, NF-kB (Coskun et al., 2011) and increase the expression of pro-inflammatory cytokines (Pestka et al., 2004).

DON-induced increased IL-8 secretion by Caco-2 cell layers was eliminated by co-exposure to MAPK p38 inhibitor SB203580, JNK1/2 inhibitor SP600125 and ERK1/2 inhibitor U0126. Co-exposure of these MAPK inhibitors inhibit the inflammatory signals as shown before (Zhang et al., 2020). Our results confirm that DON induces IL-8 secretion by Caco-2 cells via MAPK activation. Similar studies showed that DON increased the mRNA expression of IL-1, TNFα, IL-6, IL-12 and IL-15 genes in porcine IPEC-J2 cells. The increase in these pro-inflammatory genes was eliminated by the MAPK p38 inhibitor SB203580, JNK1/2 inhibitor SP600125 or ERK1/2 inhibitor U0126 (Zhang et al., 2020). Chung et al.(2003) also reported that the p38 inhibitor SB203580 or JNK1/2 inhibitor SP600125 dose-dependently decreased the expression of TNFα reporter gene in RAW 264.7 cells following DON exposure (Chung et al., 2003).

Inflammation influences bile acid reabsorption in the intestine. In our results, pre-exposure to the pro-inflammatory cytokine TNFα dose-dependently decreased TCA transport across Caco-2 cell layers. It has been shown that TNFα dose-dependently activated inflammatory signals and induced IL-8 secretion in differentiated Caco-2 cells (Van De Walle et al., 2010). In humans with an inflamed intestinal epithelium, plasma bile acid concentrations are affected (Nishida et al., 1982; Rutgeerts et al., 1979). While in healthy individuals 3.01 % of the total plasma bile acid is present as TCA, this is significantly reduced to 1.31 % and 0.9 % in patients with inactive and active Crohn's Disease (Wilson et al., 2020). Significant reductions of GCDCA, CA, GDCA, LCA and TLCA plasma concentrations were also found in patients with Crohn's ileitis

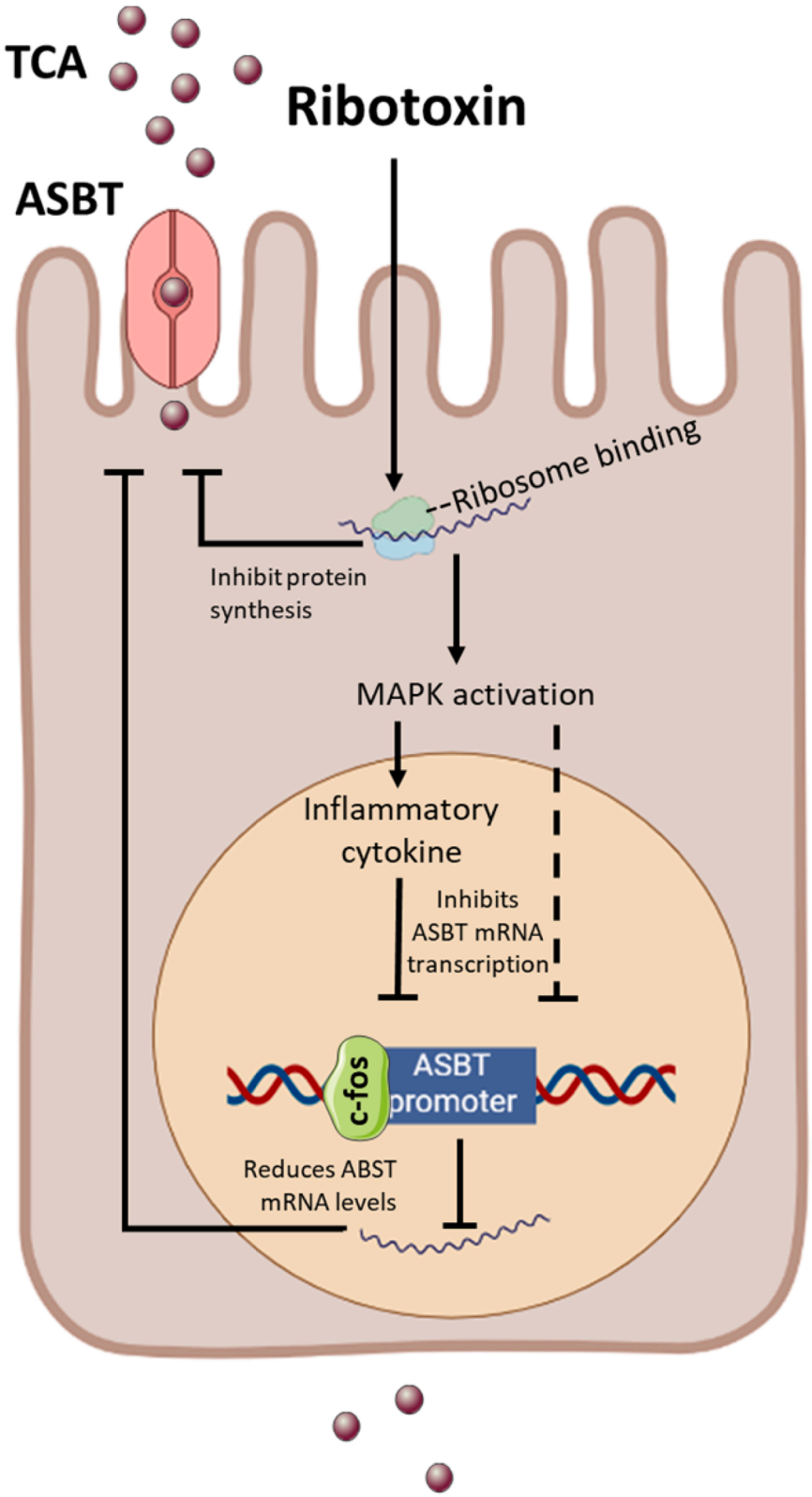

Fig. 6. Proposed mode of action of ribotoxin reducing TCA transport. Solid arrows indicate increasing effects while black bar-headed lines indicate inhibition effects, the dashed arrow indicates an potential alternative pathway.

(Wilson et al., 2020). It was assumed that the decreased plasma conjugated bile acids in patients with Crohn's disease were because of the decreased bile acid reabsorption from intestine (Vítek, 2015). To stimulate inflammation, numerous studies have utilized the "cytomix" cocktail to develop inflamed intestinal models, which is characterized by a compromised barrier that is not suitable for transport studies (Kämpfer et al., 2017). In our study, we assessed the paracellular fluorescein transport across the TNFα pre-treated Caco-2 cell layers and observed that it was below 5 %, indicating a intact intestinal epithelial barrier in the TNFα induced inflamed cell layers. Our results confirmed

this hypothesis by using an in vitro model with TNFα pre-treated Caco-2 cell layers. The TCA affinity measured by apparent Michaelis constant (K_m) for apical transporter ASBT is 4.39 μM while the TCA K_m for basolateral transporter OST is larger than 10,000 μM (Balakrishnan et al., 2006; Suga et al., 2019). It indicates the decreased bile acid reabsorption is a result from the decreased transporter expression of the apical bile acid transporter ASBT under physiological conditions (Dawson, 2017). Clinical human studies revealed that ASBT mRNA expression was significantly lower in IBD patients (Wojtal et al., 2009). *In vitro* studies found that the promoter activity of ASBT decreased in Caco-2 and IEC-6 cells following pro-inflammatory cytokines TNFα and IL-1β exposure (Chen et al., 2002).

Our results indicated a decreased ASBT mRNA expression upon DON exposure. Considering that DON induces the secretion of inflammatory cytokines via the MAPK activation, we next found that DON cannot decrease ASBT mRNA expression upon MAPK inhibition. Notably, the co-exposure of DON with MAPK inhibitors (thus blocking the inflammatory route) even increased ASBT mRNA expression while MAPK inhibitors alone did not influence the ASBT mRNA expression. This can be explained by the dual effect of DON, firstly reducing ASBT mRNA transcription via the MAPK pathway and secondly that DON increases ASBT mRNA transcription via an as yet unidentified MAPK-independent pathway. It has been shown before that the pro-inflammatory cytokine IL-1β decreased ASBT promoter activity and ASBT mRNA expression (Chen et al., 2002; Neimark et al., 2006). The cytokine effect on ASBT promotor activity is mediated via c-fos which is a downstream transcription factor of the MAPK pathway (Coskun et al., 2011; Silvers et al., 2003). It was shown that c-fos antisense treatment increased ASBT promoter activity (Neimark et al., 2006). In addition, pro-inflammatory cytokines activate the c-fos/c-jun pathway thereby inhibiting ASBT mRNA transcription (Chen et al., 2002). Following inhibition the MAPK pathway (by MAPK inhibitors), DON exposure did not decrease the ASBT mRNA transcription in our study, contrary it increased the ASBT mRNA expression. This can be explained by considering the second effect of DON, which is to increase the ASBT mRNA transcription via a MAPK-independent pathway. Apparently DON exposure induces a compensatory transcription of ASBT mRNA induced by a DON-induced ASBT protein reduction as DON decreases protein production via its effect on ribosomes (Pierron et al., 2016). ASBT is a short-lived protein with half-life of 6 h (Xia et al., 2004), as DON inhibits protein synthesis, it inhibits ASBT protein renewal which reduces ASBT protein levels in the cells. This will be compensated by the cell by increasing the ASBT mRNA transcription. This normally cannot be observed in the presence of DON because of the dual effect of DON inducing increased cytokine levels that inhibit ASBT mRNA transcription via MAPK pathways while also increasing ASBT mRNA expression via this compensatory mechanism in a MAPK independent manner, cancelling one another. However this MAPK independent DON induced increased mRNA expression becomes apparent upon blocking the MAPK pathway mediated inhibition, allowing the cell to respond with an increased mRNA transcription in response to a DON induced inhibition of protein synthesis in the presence of MAPK inhibitors. Similar to our results, Neimark et al. (2006) also reported an unexpected increase in ASBT mRNA expression upon exposure IL-1β with c-fos antisense, which even further increased ASBT promoter activity compared with c-fos antisense alone (Neimark et al., 2006). On the protein level, IL-1β induces ubiquitination and disposal of ASBT protein, which decreases ASBT protein levels and thereby inducing the compensatory transcription of ASBT mRNA upon c-fos antisense (Xia et al., 2004). Together, these results suggest that DON exposure decreases ASBT mRNA expression by activating the MAPK pathway, which masks an up-regulatory effect of DON on ASBT mRNA expression via a DON-induced reduction of ASBT protein synthesis.

The apical bile acid transporter ASBT actively transports TCA across the apical brush border membrane of intestinal epithelial cells from the intestinal lumen. DON decreased ASBT mRNA expression while co-exposure of MAPK inhibitors with DON increased ASBT mRNA expression. However, similar amounts of TCA were transported across Caco-2 cell layers upon pre-exposure to DON or DON + MAPK inhibitors, which was significantly lower than that following the pre-exposure to solvent control or MAPK inhibitors alone. The paracellular fluorescein transport among the different pre-exposure groups were similar. It indicates that the difference of TCA transport is because of the different transcellular TCA transport among the DON pre-exposure groups.

Upon exposure, DON binds to ribosomes which is the upstream event of MAPK activation and subsequently results in inhibited protein translation (Pestka, 2010). Thus, we hypothesize that protein inhibition results in the reduced TCA transport across Caco-2 cell layers. To confirm this hypothesis, the protein content is quantified following DON exposure. The results showed that DON dose-dependently decreased protein content and the reduction showed statistical significance at 2.5 μM, which is the DON concentration used in the TCA transport study. DON forms three hydrogen bonds with the A-site of the peptidyl transferase centre in the 60 S subunit of the ribosome and interferes with the elongation step of protein translation, which inhibits the protein synthesis (Davis, 1987; Pierron et al., 2016). The ribotoxin cycloheximide exhibits a similar mode of action as DON at the molecular level, targeting the ribosome and inhibiting protein translation (Shen et al., 2021). Cycloheximide is a widely used laboratory inhibitor of eukaryotic protein synthesis without inducing pro-inflammatory cytokines secretion (Schneider-Poetsch et al., 2010). In our results, the decreased protein content and reduced TCA transport were found in Caco-2 cell layers without increasing IL-8 secretion following cycloheximide exposure. In addition, more non-inflammatory ribotoxins such as tobramycin, have been found to reduce TCA transport across Caco-2 cell layers (Zhang et al., 2022). The similarity between the activity of these ribotoxins on decreased TCA transport was consistent with their common ability to inhibit protein synthesis. Together, it suggests that the binding to the ribosome and the resulting inhibition of protein synthesis can be the molecular initiating events for the adverse outcome of bile acid malabsorption.

5. Conclusion

Our study sheds light on the mechanism of the effect of ribotoxin DON on reduced TCA transport across Caco-2 cell layers. Firstly, DON induces pro-inflammatory cytokine IL-8 expression in Caco-2 cells. Inflammatory cytokines are downstream factors of MAPK pathways, supported by the fact that MAPK inhibitors eliminate IL-8 secretion induced by DON. Inflammation has been shown to decrease ASBT mRNA expression. We further confirmed that TCA transport decreased across TNFα-pretreated Caco-2 cell layers used as a model to represent inflamed intestinal epithelia. Moreover, we found that DON decreased ASBT mRNA expression while MAPK inhibitors prevented this down-regulatory effect of DON. Together, this indicates a central role of the MAPK pathway via inflammatory cytokines on the downregulation of ASBT gene expression upon DON exposure. However, we cannot rule out a parallel pathway in which MAPK activation directly affects ASBT gene expression. Finally, we found that DON-induced TCA transport reduction was not eliminated by MAPK inhibitors. Non-inflammatory ribotoxin cycloheximide inhibited protein synthesis and reduce TCA transport across Caco-2 cell layers. Together, this study suggested that the DON-induced TCA malabsorption is regulated by MAPK activation and protein synthesis inhibition, both of which are initiated by the ribosomes binding activity which therefore is the molecular initiating event for the adverse outcome of bile acid malabsorption in the intestine.

Ethical approval

Not applicable.

Funding

This work was supported by a grant from the China Scholarship Council, China (No. 201906350086) to Jingxuan Wang.

CRediT authorship contribution statement

JW, LH, HB contributed to the study conception and design. WB contributed to optimize the LC-MS method for the quantification bile acids. JW and BS conducted all of the experimental work. Writing-original draft preparation: JW, HB; Writing-review and editing: JW and HB.

Declaration of Competing Interest

The authors declare that they have no known competing financial interests or personal relationships that could have appeared to influence the work reported in this paper.

Data Availability

Data will be made available on request.

Acknowledgements

The authors gratefully acknowledge prof.dr.ir. Jacques Vervoort and Weijia Zheng for optimizing the LC-MS methods for the quantification of bile acids. The authors thank Tisha Moni Punom for helping with the cell culture. The authors thank Prof.dr.ir. Ivonne. M.C.M. Rietjens for critically commenting the work described here.

Appendix A. Supporting information

Supplementary data associated with this article can be found in the online version at doi:10.1016/j.toxlet.2023.06.001.

References

Alrefai, W.A., Gill, R.K., 2007. Bile acid transporters: structure, function, regulation and pathophysiological implications. Pharm. Res. 24, 1803–1823.
Balakrishnan, A., Wring, S.A., Polli, J.E., 2006. Interaction of native bile acids with human apical sodium-dependent bile acid transporter (hASBT): influence of steroidal hydroxylation pattern and C-24 conjugation. Pharm. Res. 23, 1451–1459.
Cano, P.M., Seeboth, J., Meurens, F., Cognie, J., Abrami, R., Oswald, I.P., Guzylack-Piriou, L., 2013. Deoxynivalenol as a new factor in the persistence of intestinal inflammatory diseases: an emerging hypothesis through possible modulation of Th17-mediated response. PLoS One 8, e53647.
Chen, F., Lin, M., Sartor, R.B., Li, F., Xiong, H., Sun, A.Q., Shneider, B., 2002. Inflammatory-mediated repression of the rat ileal sodium-dependent bile acid transporter by c-fos nuclear translocation. Gastroenterology 123, 2005–2016.
Chung, Y.-J., Zhou, H.-R., Pestka, J.J., 2003. Transcriptional and posttranscriptional roles for p38 mitogen-activated protein kinase in upregulation of TNF-α expression by deoxynivalenol (vomitoxin). Toxicol. Appl. Pharmacol. 193, 188–201.
Coskun, M., Olsen, J., Seidelin, J.B., Nielsen, O.H., 2011. MAP kinases in inflammatory bowel disease. Clin. Chim. Acta 412, 513–520.
Davis, B.D., 1987. Mechanism of bactericidal action of aminoglycosides. Microbiol. Rev. 51, 341–350.
Dawson, P.A., 2017. Roles of ileal ASBT and OSTα-OSTβ in regulating bile acid signaling. Dig. Dis. 35, 261–266.
Dawson, P.A., Lan, T., Rao, A., 2009. Bile acid transporters. J. Lipid Res. 50, 2340–2357.
Chain, EFSA, Knutsen, E.Po.CitF., Alexander, H.K., Barregård, J., Bignami, L., Brüschweiler, M., Ceccatelli, B., Cottrill, S., Dinovi, B., Grasl-Kraupp, B, M., 2017. Risks to human and animal health related to the presence of deoxynivalenol and its acetylated and modified forms in food and feed. EFSA J. 15, e04718.
Ge, L., Lin, Z., Le, G., Hou, L., Mao, X., Liu, S., Liu, D., Gan, F., Huang, K., 2020. Nontoxic-dose deoxynivalenol aggravates lipopolysaccharides-induced inflammation and tight junction disorder in IPEC-J2 cells through activation of NF-κB and LC3B. Food Chem. Toxicol. 145, 111712.
Heubi, J.E., Balistreri, W.F., Fondacaro, J.D., Partin, J.C., Schubert, W.K., 1982. Primary bile acid malabsorption: defective in vitro ileal active bile acid transport. Gastroenterology 83, 804–811.
Hou, S., Ma, J., Cheng, Y., Wang, H., Sun, J., Yan, Y., 2021. The toxicity mechanisms of DON to humans and animals and potential biological treatment strategies. Crit. Rev. Food Sci. Nutr. 1–23.
Jahnel, J., Fickert, P., Hauer, A.C., Högenauer, C., Avian, A., Trauner, M., 2014. Inflammatory bowel disease alters intestinal bile acid transporter expression. Drug Metab. Dispos. 42, 1423–1431.
JECFA, 2011. Safety evaluation of certain contaminants in food. prepared by the Seventy-second meeting of the Joint FAO/WHO Expert Committee on Food Additives (JECFA). World Health Organization.
Jia, W., Xie, G., Jia, W., 2018. Bile acid–microbiota crosstalk in gastrointestinal inflammation and carcinogenesis. Nat. Rev. Gastroenterol. Hepatol. 15, 111–128.
Kadota, T., Furusawa, H., Hirano, S., Tajima, O., Kamata, Y., Sugita-Konishi, Y., 2013. Comparative study of deoxynivalenol, 3-acetyldeoxynivalenol, and 15-acetyldeoxynivalenol on intestinal transport and IL-8 secretion in the human cell line Caco-2. Toxicol. Vitr. 27, 1888–1895.
Kämpfer, A.A., Urbán, P., Gioria, S., Kanase, N., Stone, V., Kinsner-Ovaskainen, A., 2017. Development of an in vitro co-culture model to mimic the human intestine in healthy and diseased state. Toxicol. Vitr. 45, 31–43.
Laskin, J.D., Heck, D.E., Laskin, D.L., 2002. The ribotoxic stress response as a potential mechanism for MAP kinase activation in xenobiotic toxicity. Toxicol. Sci. 69, 289–291.
Li, M., Vokral, I., Evers, B., de Graaf, I.A., de Jager, M.H., Groothuis, G.M., 2018. Human and rat precision-cut intestinal slices as ex vivo models to study bile acid uptake by the apical sodium-dependent bile acid transporter. Eur. J. Pharm. Sci. 121, 65–73.
Maresca, M., 2013. From the gut to the brain: journey and pathophysiological effects of the food-associated trichothecene mycotoxin deoxynivalenol. Toxins 5, 784–820.
Maresca, M., Fantini, J., 2010. Some food-associated mycotoxins as potential risk factors in humans predisposed to chronic intestinal inflammatory diseases. Toxicon 56, 282–294.
Mishra, S., Tripathi, A., Chaudhari, B.P., Dwivedi, P.D., Pandey, H.P., Das, M., 2014. Deoxynivalenol induced mouse skin cell proliferation and inflammation via MAPK pathway. Toxicol. Appl. Pharmacol. 279, 186–197.
Neimark, E., Chen, F., Li, X., Magid, M.S., Alasio, T.M., Frankenberg, T., Sinha, J., Dawson, P.A., Shneider, B.L., 2006. c-Fos is a critical mediator of inflammatory-mediated repression of the apical sodium-dependent bile acid transporter. Gastroenterology 131, 554–567.
Nishida, T., Miwa, H., Yamamoto, M., Koga, T., Yao, T., 1982. Bile acid absorption kinetics in Crohn's disease on elemental diet after oral administration of a stable-isotope tracer with chenodeoxycholic-11, 12-d2 acid. Gut 23, 751–757.
Payros, D., Alassane-Kpembi, I., Pierron, A., Loiseau, N., Pinton, P., Oswald, I.P., 2016. Toxicology of deoxynivalenol and its acetylated and modified forms. Arch. Toxicol. 90, 2931–2957.
Pestka, J.J., 2010. Deoxynivalenol-induced proinflammatory gene expression: mechanisms and pathological sequelae. Toxins 2, 1300–1317.
Pestka, J.J., Zhou, H.-R., Moon, Y., Chung, Y., 2004. Cellular and molecular mechanisms for immune modulation by deoxynivalenol and other trichothecenes: unraveling a paradox. Toxicol. Lett. 153, 61–73.
Pfaffl, M.W., 2001. A new mathematical model for relative quantification in real-time RT–PCR. Nucleic Acids Res. 29 e45-e45.
Pierron, A., Mimoun, S., Murate, L.S., Loiseau, N., Lippi, Y., Bracarense, A.-P.F., Schatzmayr, G., He, J.W., Zhou, T., Moll, W.-D., 2016. Microbial biotransformation of DON: molecular basis for reduced toxicity. Sci. Rep. 6, 1–13.
Reimund, J.-M., Wittersheim, C., Dumont, S., Muller, C., Baumann, R., Poindron, P., Duclos, B., 1996. Mucosal inflammatory cytokine production by intestinal biopsies in patients with ulcerative colitis and Crohn's disease. J. Clin. Immunol. 16, 144–150.
Rutgeerts, P., Ghoos, Y., Vantrappen, G., 1979. Bile acid studies in patients with Crohn's colitis. Gut 20, 1072–1077.
Schneider-Poetsch, T., Ju, J., Eyler, D.E., Dang, Y., Bhat, S., Merrick, W.C., Green, R., Shen, B., Liu, J.O., 2010. Inhibition of eukaryotic translation elongation by cycloheximide and lactimidomycin. Nat. Chem. Biol. 6, 209–217.
Schuerer-Maly, C., Eckmann, L., Kagnoff, M., Falco, M., Maly, F., 1994. Colonic epithelial cell lines as a source of interleukin-8: stimulation by inflammatory cytokines and bacterial lipopolysaccharide. Immunology 81, 85.
Sergent, T., Parys, M., Garsou, S., Pussemier, L., Schneider, Y.-J., Larondelle, Y., 2006. Deoxynivalenol transport across human intestinal Caco-2 cells and its effects on cellular metabolism at realistic intestinal concentrations. Toxicol. Lett. 164, 167–176.
Shen, L., Su, Z., Yang, K., Wu, C., Becker, T., Bell-Pedersen, D., Zhang, J., Sachs, M.S., 2021. Structure of the translating Neurospora ribosome arrested by cycloheximide. Proc. Natl. Acad. Sci. 118.
Siegel, M.R., Sisler, H.D., 1963. Inhibition of protein synthesis in vitro by cycloheximide. Nature 200, 675–676.
Silvers, A.L., Bachelor, M.A., Bowden, G.T., 2003. The role of JNK and p38 MAPK activities in UVA-induced signaling pathways leading to AP-1 activation and c-Fos expression. Neoplasia 5, 319–329.
Sonnier, D.I., Bailey, S.R., Schuster, R.M., Lentsch, A.B., Pritts, T.A., 2010. TNF-α induces vectorial secretion of IL-8 in Caco-2 cells. J. Gastrointest. Surg. 14, 1592–1599.
Suga, T., Yamaguchi, H., Ogura, J., Mano, N., 2019. Characterization of conjugated and unconjugated bile acid transport via human organic solute transporter α/β. Biochim. Et. Biophys. Acta (BBA)-Biomembr. 1861, 1023–1029.
Van De Walle, J., Hendrickx, A., Romier, B., Larondelle, Y., Schneider, Y.-J., 2010. Inflammatory parameters in Caco-2 cells: effect of stimuli nature, concentration, combination and cell differentiation. Toxicol. Vitr. 24, 1441–1449.
Van De Walle, J., Romier, B., Larondelle, Y., Schneider, Y.-J., 2008. Influence of deoxynivalenol on NF-κB activation and IL-8 secretion in human intestinal Caco-2 cells. Toxicol. Lett. 177, 205–214.
Vignal, C., Djouina, M., Pichavant, M., Caboche, S., Waxin, C., Beury, D., Hot, D., Gower-Rousseau, C., Body-Malapel, M., 2018. Chronic ingestion of deoxynivalenol at

human dietary levels impairs intestinal homeostasis and gut microbiota in mice. Arch. Toxicol. 92, 2327–2338.
Vítek, L., 2015. Bile acid malabsorption in inflammatory bowel disease. Inflamm. bowel Dis. 21, 476–483.
Wang, J., Bakker, W., Zheng, W., de Haan, L., Rietjens, I.M., Bouwmeester, H., 2022. Exposure to the mycotoxin deoxynivalenol reduces the transport of conjugated bile acids by intestinal Caco-2 cells. Arch. Toxicol. 1–10.
Wilson, A., Almousa, A., Teft, W.A., Kim, R.B., 2020. Attenuation of bile acid-mediated FXR and PXR activation in patients with Crohn's disease. Sci. Rep. 10, 1–11.
Wojtal, K.A., Eloranta, J.J., Hruz, P., Gutmann, H., Drewe, J., Staumann, A., Beglinger, C., Fried, M., Kullak-Ublick, G.A., Vavricka, S.R., 2009. Changes in mRNA expression levels of solute carrier transporters in inflammatory bowel disease patients. Drug Metab. Dispos. 37, 1871–1877.
Xia, X., Roundtree, M., Merikhi, A., Lu, X., Shentu, S., LeSage, G., 2004. Degradation of the apical sodium-dependent bile acid transporter by the ubiquitin-proteasome pathway in cholangiocytes. J. Biol. Chem. 279, 44931–44937.
Zhang, H., Deng, X., Zhou, C., Wu, W., Zhang, H., 2020. Deoxynivalenol induces inflammation in IPEC-J2 cells by activating P38 Mapk and Erk1/2. Toxins 12, 180.
Zhang, N., Wang, J., Bakker, W., Zheng, W., Baccaro, M., Murali, A., van Ravenzwaay, B., Rietjens, I.M., 2022. In vitro models to detect in vivo bile acid changes induced by antibiotics. Arch. Toxicol. 96, 3291–3303.